Imaging of Malignant Bone Involvement by Morphologic, Scintigraphic, and Hybrid Modalities*

Einat Even-Sapir, MD, PhD

Department of Nuclear Medicine, Tel Aviv Sourasky Medical Center, Sackler School of Medicine, Tel Aviv University, Tel Aviv, Israel

Detection of bone involvement is essential for optimal therapy of oncologic patients. The purpose of imaging is to identify early bone involvement, to determine the full extent of the skeletal disease, to assess the presence of accompanying complications—such as fractures and cord compression—and to monitor response to therapy. Detection of bone involvement by various imaging modalities is based on either direct visualization of tumor infiltration or detection of the reaction of bone to the malignant process. MRI can identify early involvement of bone marrow. CT, which depends mainly on bone destruction, provides detailed bone morphology. In nuclear medicine, uptake of ^{18}F-FDG is directly into tumor cells, thus allowing for early detection and monitoring the response to therapy of tumor sites in the marrow, bone, and soft tissue, whereas increased uptake of ^{18}F-fluoride and ^{99m}Tc-methylene diphosphonate reflects the osteoblastic reaction of bone to the presence of tumor cells. The hybrid techniques SPECT/CT and PET/CT, recently introduced into clinical practice, provide a better anatomic localization of scintigraphic findings and may improve the diagnostic accuracy of SPECT and PET in detecting malignant bone involvement. The current review discusses the basis for the detection of malignant bone involvement by various morphologic and scintigraphic imaging modalities and the advantages and the limitations of each. Special emphasize is placed on the newer integrated technique of PET/CT. The role of imaging in identifying bone involvement in different malignant diseases is also discussed.

J Nucl Med 2005; 46:1356–1367

Bone metastases are the most common malignant bone tumor. Skeletal involvement occurs in 30%–70% of all cancer patients, with breast cancer being the leading cause for bone metastases in women and prostate cancer in men, followed by lung cancer (*1*). Detection of tumor bone metastases is essential for optimal therapy (*2*). The purpose of imaging is to identify bone metastases as early as possible, to determine the full extent of disease, to evaluate the presence of complications that may accompany malignant bone involvement (including pathologic fractures and spinal cord compression), to monitor response to therapy, and, occasionally, to guide biopsy if histologic confirmation is indicated (*1,2–4*).

Bone consists of cortical, trabecular, and marrow components (*4*). Bone involvement by cancer occurs most commonly by hematogenous spread. The venous system is the main pathway for transport of tumor cells to the skeleton, although tumor may occasionally extend directly from the soft tissue to the adjacent bone (*5*). The vast majority of bone metastases initiate as intramedullary lesions (Figs. 1A and 1B). Over 90% of bone metastases are found in the distribution of the red active marrow, which is located in the axial skeleton, in adults (*1,4,6*). The normal bone undergoes constant remodeling, maintaining a balance between osteoclastic (resorptive) and osteoblastic activity. As the metastatic lesion enlarges within the marrow, the surrounding bone undergoes osteoclastic and osteoblastic reactive changes. Based on the balance between the osteoclastic and osteobalstic processes, the radiographic appearance of a bone metastasis may be lytic, sclerotic (blastic), or mixed (Figs. 1C–1F). The osteoblastic component of the metastasis represents reaction of normal bone to the metastatic process. Rapidly growing aggressive metastases tend to be lytic, whereas sclerosis is considered to indicate a slower tumor growth rate. Sclerosis may also be a sign of repair after treatment (*1,7,8*).

The incidence of lytic, blastic, and mixed types of bone metastases is different in various tumor types. Lytic lesions may be seen in almost all tumor types. Bone metastases of bladder, kidney, and thyroid cancer and lesions of multiple myeloma are invariably lytic. Blastic lesions are frequently seen in prostate and breast cancer, occasionally in lung, stomach, pancreas, and cervix carcinomas, and infrequently in colorectal cancer (*1*).

Many patients with bone metastases are asymptomatic and metastases are detected incidentally on routine screen-

Received Feb. 27, 2005; revision accepted May 9, 2005.

For correspondence or reprints contact: Einat Even-Sapir, MD, PhD, Department of Nuclear Medicine, Tel-Aviv Sourasky Medical Center, 6 Weizman St., Tel-Aviv, 64239 Israel.

E-mail: evensap@tasmc.health.gov.il

*NOTE: FOR CE CREDIT, YOU CAN ACCESS THIS ACTIVITY THROUGH THE SNM WEB SITE (http://www.snm.org/ce_online.html) THROUGH AUGUST 2006.

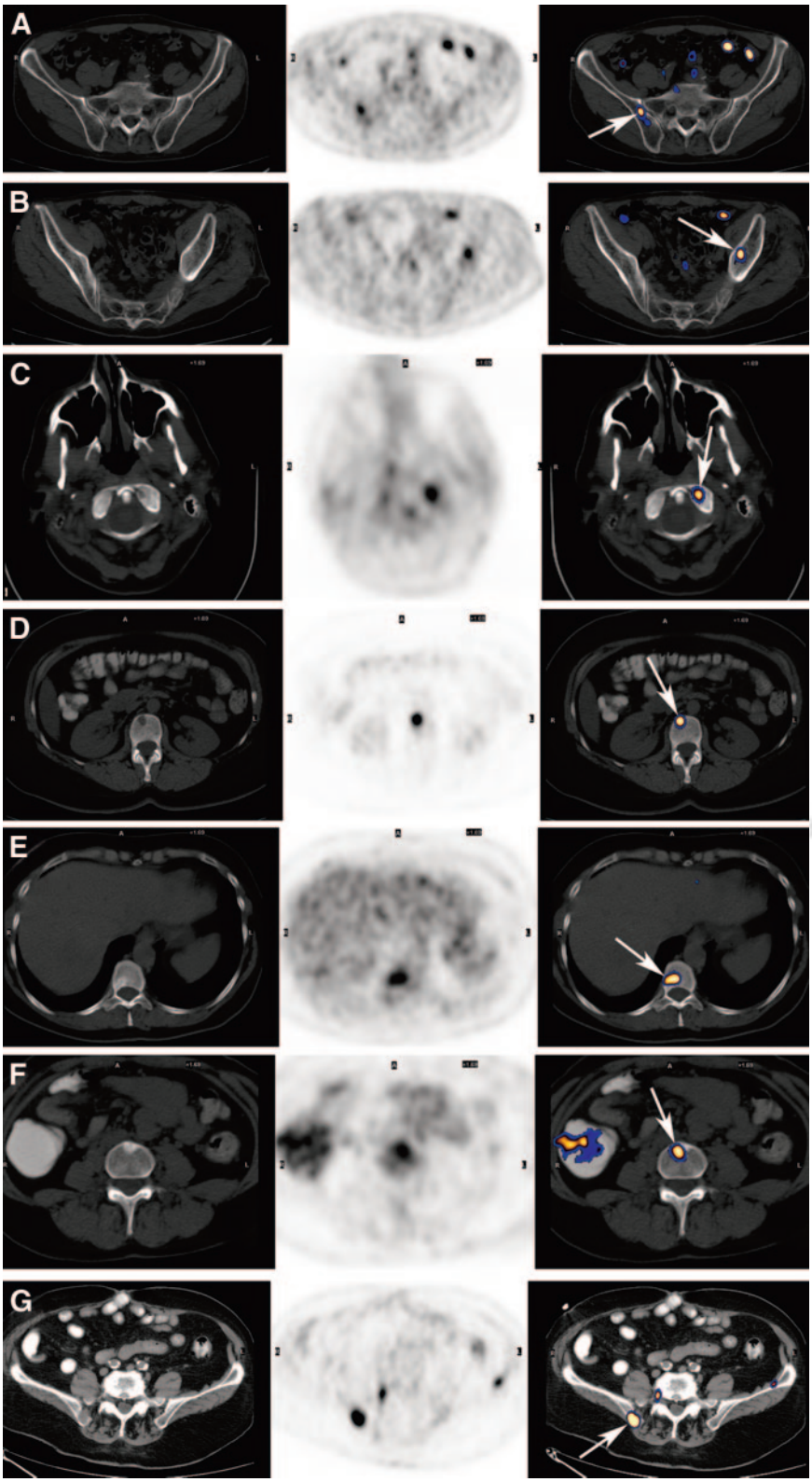

FIGURE 1. Different patterns of CT appearance in ^{18}F-FDG–avid bone metastases. Each row represents another metastasis. From left to right: CT image, ^{18}F-FDG PET image, and fused image. Metastases are marked by arrows. (A) CT appearance is normal on early bone marrow metastasis. (B) Early bone marrow metastasis. Minimal asymmetry is detected on CT. Involved marrow is more attenuated than normal marrow. (C) Lytic metastasis. Minor lytic changes are detected on CT at left occipital condyle. This finding was overlooked when CT was interpreted without PET. (D) Lytic lesion. A lytic lesion is clearly detected on CT. (E) Mixed lytic sclerotic metastasis. Location of lesion in posterior part of vertebral body, next to region of pedicle, is characteristic of early vertebral malignant involvement and is caused by its proximity to vertebral venous network. (F) Sclerotic metastasis. (G) Lytic metastasis with soft-tissue component. Margins of bone are disrupted and soft-tissue mass is discernible.

ing or when a cause for rising tumor markers is looked for. Symptoms occur mainly when the lesion increases in size, causing extensive bone destruction, which may lead to collapse or fracture, or in the presence of accompanying complications, such as spinal cord compression or nerve root invasion (Fig. 2) (*9*).

There are various morphologic and functional imaging modalities for the assessment of malignant bone involve-

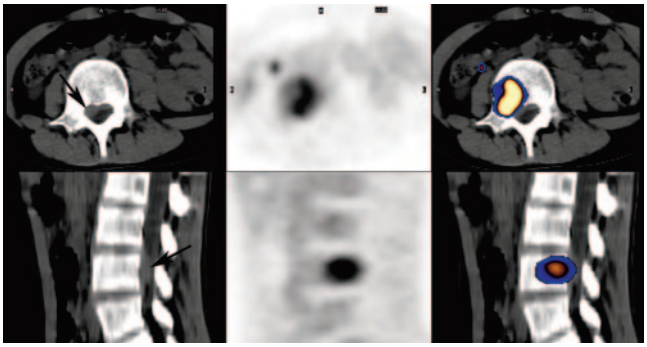

FIGURE 2. Detection of accompanying epidural mass by ^{18}F-FDG PET/CT in patient with lymphoma. Top row, transaxial images; bottom row, sagittal images. From left to right: CT image, ^{18}F-FDG PET image, and fused image. Tumor is marked by arrows. Based on fusion with CT, increased ^{18}F-FDG uptake is detected in right aspect of L4 and in accompanying epidural component. Soft-tissue epidural mass appears to displace the thecal sac laterally, on CT.

ment, including plain radiography (XR), CT, MRI, bone scintigraphy (BS), PET with ^{18}F-FDG or ^{18}F-fluoride, and, recently, integrated SPECT/CT and PET/CT.

XR, CT, AND MRI

Conventional XR is appropriate for imaging abnormalities of cortical and trabecular bone by detecting lytic, sclerotic, and mixed-type lesions. It provides only minimal data on the integrity of the bone marrow (*2*). The main limitation of XR in imaging malignant bone involvement is that considerable bone destruction must be present before a bone metastasis is evident radiographically. It has been estimated that 30%–75% reduction in bone density is required to visualize a metastasis on XR. Therefore, the detection of a metastasis may be delayed by several months compared with other bone modalities, such as BS (*1,2,4*).

The advantage of CT is its good anatomic resolution, soft-tissue contrast, and detailed morphology. Both cortical and trabecular bone components are well defined. The sensitivity of CT for detecting bone metastasis ranges between 71% and 100% (*4*). Because considerable cortical destruction is required for visualization of a metastasis by CT, the sensitivity of this modality in detecting early malignant bone involvement is relatively low (*10*). Moreover, cortical destruction may be especially difficult to determine in the presence of severe osteoporotic or degenerative changes (*11*). CT is not sensitive for assessment of malignant marrow infiltration, although the presence of the latter may occasionally be suggested because marrow infiltrated by tumor cells is more attenuated compared with normal marrow (Figs. 1A and 1B) (*12*).

CT is not a routine modality for survey of metastatic bone involvement but, when included in the staging algorithm, such as in patients with newly diagnosed non–small cell lung cancer (NSCLC), bone metastases may found incidentally. CT is commonly used for further assessment of equivocal lesions suggested by BS and has an important role in identifying complications that may accompany malignant bone involvement, such as fractures and spinal cord compression or neural foramen involvement (in the case of vertebral metastases). CT can assist in differentiating malignant from benign vertebral collapse. The detection of an accompanying soft-tissue mass or involvement of posterior vertebral body elements often suggests a malignant nature (Figs. 1G and 2). The appropriate route for taking a bone biopsy can also be defined on CT as well as the presence of a soft-tissue component that may be easier to sample (*13*).

MRI has good spatial and contrast resolution. It is an optimal imaging modality for bone marrow assessment and is able to separate hematopoetic marrow (red) from nonhematopoetic marrow (yellow). MRI can detect an early intramedullary malignant lesion before there is any cortical destruction or reactive processes. Normal marrow shows a high-intensity signal on T1-weighted imaging, whereas metastases appear as areas of reduced signal, reflecting the replacement of fat in the marrow by tumor. Bone marrow metastases have longer T1- and T2-weighted relaxation time than normal marrow and are usually enhanced after the administration of contrast medium. MRI can detect bone marrow metastases missed by BS (*14*). Detection of malignant marrow infiltration by MRI is better than by CT. Moreover, MRI has a better contrast resolution for visualizing soft-tissue and spinal cord lesions and, thus, is superior to CT in differentiating benign and malignant causes of spinal cord compression and vertebral compression fracture (*11*). However, MRI is less sensitive than CT for detecting cortical bone destruction because cortical bone appears black on T1- and T2-weighted sequences (*12*). The specificity of MRI is moderate because of overlap in the appearance of metastases and a variety of benign lesions. In the vertebral column, for instance, benign lesions, which may be confused with metastases, include degenerative disk disease, osteomyelitis, a benign compression fracture, infarcts, and Schmorl's nodes. An abnormal signal in the posterior aspect of the vertebral body extending into the posterior elements suggests a malignant nature. When MRI is performed in young adults, highly cellular malignancy needs to be differentiated from hematopoietic marrow, which shows age-dependent variability (*15*). It might be difficult to differentiate between active disease and scar, necrosis, or fracture when monitoring the response to therapy by MRI (*14*). Currently, the use of MRI is mainly reserved for regional assessment of a bone lesion suggested by BS or CT (*13,14*). New MRI coils and sequences, which allow the performance of whole-body MRI in a reasonable acquisition time, have been recently introduced (*15,16*). This whole-body modality, however, is not a routine technique and its role in assessing malignant bone involvement in cancer patients is yet to be determined.

BS

BS is the most commonly used modality for detection of bone metastases because it is widely available and provides an entire skeletal visualization within a reasonable amount of time and cost (*4,7,13*). ^{99m}Tc-Methylene diphosphonate (^{99m}Tc-MDP) is the most commonly used tracer for skeletal imaging in general nuclear medicine. In contrast with XR, as little as a 5%–10% change in the ratio of lesion to normal bone is required to detect an abnormality on BS (*1,7*). It has been estimated that BS can detect malignant bone lesions 2–18 mo earlier than XR (*1*). BS is, therefore, the initial imaging modality in cancer patients who are at high risk for bone metastases, for example, those with advanced-stage breast or prostate cancer. Published sensitivity rates of BS in detecting bone metastases vary between 62% and 100% with a specificity of 78%–100% (*4*).

As for the mechanism of increased ^{99m}Tc-MDP uptake in malignant bone involvement, it is believed that the compound is chemisorbed onto bone surface. Its uptake reflects skeletal metabolic activity and depends on the local blood flow and osteoblastic activity (*3,7,13*). Most sites of malignant bone involvement show reactive increased osteoblastic activity and, therefore, increased ^{99m}Tc-MDP uptake. BS is reliable for detecting metastases from breast, prostate, and lung cancer. It is less sensitive in detecting tumor types, which are associated with predominately lytic bone lesions with no or only minimal osteoblastic reaction, such as multiple myeloma or aggressive metastatic lesions with rapid bone destruction. Lytic lesions may appear "cold" on BS but are not uncommonly overlooked. Widespread metastatic involvement can give rise to a "superscan," characterized by a uniform distribution of ^{99m}Tc-MDP, a high ratio of bone to soft-tissue activity, and, usually, nonvisualization of kidneys (*1*).

After therapy, healing may be indicated by a decrease in the intensity of uptake or the disappearance of lesions that had been detected on a baseline study. However, insofar as the bone repair process is also associated with increased osteoblastic activity, BS may not be able to accurately differentiate between ongoing disease and complete response. The "flare phenomenon" is seen on the BS of patients receiving antihormonal therapy. It is characterized by an increase in uptake as a result of the stimulation of osteoblastic activity during the repair process. Lytic lesions that had been overlooked on BS before therapy may present as "new" sites of increased uptake and, therefore, may be misinterpreted as indicating disease progression. Thus, BS performed within the first few months after initiation of treatment must be interpreted with caution to avoid unwarranted discontinuation of treatment. Differentiation between the flare phenomenon and disease progression can be obtained based on the interval changes in the appearance of soft-tissue sites of disease on other imaging modalities, mainly CT (*17*). The time sequence of the appearance of scintigraphic alterations may validate the diagnosis of the flare phenomenon, which usually occurs during the first 3 mo after the initiation of therapy with a gradual decrease in intensity of uptake after 6 mo (*18–20*).

Despite the high sensitivity, ^{99m}Tc-MDP is not a tumor-specific tracer and increased accumulation of ^{99m}Tc-MDP may also be detected in benign bone lesions. The presence of multiple bone lesions on BS, mainly in patients with a known malignancy, is suggestive of a metastatic spread, although it should be borne in mind that there are benign conditions, which may also be multifocal, such as trauma, metabolic bone disease, ostomyelitis, osteoporosis, and others. The detection of a solitary or few bone lesions on BS often indicates the need for further assessment of the lesions. Correlation with CT is commonly performed to overcome the limited specificity of BS (*4,13*).

The addition of SPECT to the acquisition protocol of BS has been reported to improve its diagnostic accuracy for detecting malignant bone involvement and to allow for a straightforward comparison with other tomographic-based techniques such as CT and MRI. SPECT is more sensitive in detecting bone lesions than planar scintigraphy. It was reported to detect 20%–50% more lesions in the spine compared with planar BS (*21*). The sensitivity, specificity, positive predictive value, and negative predictive value of SPECT BS for the detection of bone metastases, as investigated in 118 patients by Savelli et al. were 91%, 93%, 73%, and 98%, respectively (*22*).

The possible limitation of anatomic localization of lesions on planar views by superimposition is overcome by the tomographic data of SPECT. The better localization of lesions by SPECT has been reported to improve the specificity of BS. In the vertebral column, for instance, different disease processes tend to involve different parts of the vertebra. Accurate localization of a scintigraphic lesion within the vertebra by SPECT has been reported to improve the specificity of ^{99m}Tc-MDP BS, differentiating between benign and malignant sites of uptake (*21–23*). It has been suggested that the predilection of metastatic vertebral involvement to the posterior part of the vertebral body and pedicle is secondary to the location of the vertebral venous network, which provides the route for hematogenous spread of tumor cells into the vertebra (*24*). Thus, the distinction between benign and early malignant vertebral lesion on SPECT, CT, and MRI often depends on assessment of the appearance of the posterior part of the vertebral body and pedicle (*23,25*).

The main drawback of SPECT is that data are obtained for only a limited skeletal region. In a busy routine clinical practice, it is not possible to perform several SPECT acquisitions to assess, tomographically, the entire skeleton. It may well be that future γ-cameras and software will allow for the performance of whole-body SPECT BS in a reasonable acquisition and processing time to overcome this drawback.

PET

PET is characterized by high-contrast resolution, whole-body tomographic data and the ability to perform absolute quantitation of tracer uptake. Using the various PET tracers, functional changes occurring in the bone marrow and bone as a result of malignant infiltration may precede the structural changes required to identify the presence of malignant bone involvement by morphologic imaging modalities. Measurements of the regional skeletal kinetic parameters using compartmental modeling and nonlinear regression analysis have been reported to have a role in differentiating malignant from benign lesions as well as for monitoring response to therapy (*26–30*).

The 2 PET tracers that are clinically used for assessment of malignant bone involvement are ^{18}F-fluoride and ^{18}F-FDG.

^{18}F-Fluoride PET

^{18}F-Fluoride was first introduced as a bone-imaging agent by Blau at al. in 1962 (*31*). Its uptake mechanism is similar to that of ^{99m}Tc-MDP. After diffusion through capillaries into bone extracellular fluid, fluoride ions exchange with hydroxyl groups in hydroxyapatite crystal bone to form fluoroapatite, which is deposited mainly at the surface, where bone remodeling and turnover are greatest. Similarly to ^{99m}Tc-MDP, accumulation of ^{18}F-fluoride uptake in malignant bone lesions reflects the increased regional blood flow and bone turnover characterizing these lesions. Bone uptake of ^{18}F-fluoride is 2-fold higher than that of ^{99m}Tc-MDP. It is not bound to protein, in contrast with ^{99m}Tc-MDP, which does bind to protein to an extent ranging from 25% binding immediately after injection to 70% 12 h after injection. The higher capillary permeability of ^{18}F-fluoride and its faster blood clearance result in a better target-to-background ratio. Regional plasma clearance of ^{18}F-fluoride was reported to be 3–10 times higher in bone metastases compared with that of normal bone (*7,26,30*).

Combining the better spatial resolution of PET and the favorable pharmacokinetic characteristics of ^{18}F-fluoride led previous investigators to use ^{18}F-fluoride PET in the evaluation of skeletal metastases. Increased ^{18}F-fluoride uptake may be detected in both sclerotic and lytic metastases (Fig. 3). ^{18}F-Fluoride PET is more sensitive than ^{99m}Tc-MDP BS, mainly for the detection of lytic lesions, because the minimal osteoblastic activity accompanying a lytic lesion, which may not be identified on BS, may be appropriate for detecting a lesion on ^{18}F-fluoride PET (*3,26,32*). Schirrmeister et al. reported that ^{18}F-fluoride PET detected bone metastases overlooked by BS in patients with lung cancer and that all metastatic lesions diagnosed by MRI were also detected by ^{18}F-fluoride PET (*32*). It should be noted that ^{18}F-fluoride PET was reported to be of a higher value compared with planar BS than compared with bone SPECT, reflecting the benefit of tomographic techniques (*32*).

^{18}F-Fluoride PET is not a routine imaging modality for detecting malignant bone involvement. Its use is primarily suggested in patients at high risk for metastatic bone disease—that is, if bone metastases are suspected clinically and BS is negative—and in patients with a tumor type that has predominately lytic bone lesions (*3,7,26,32,33*).

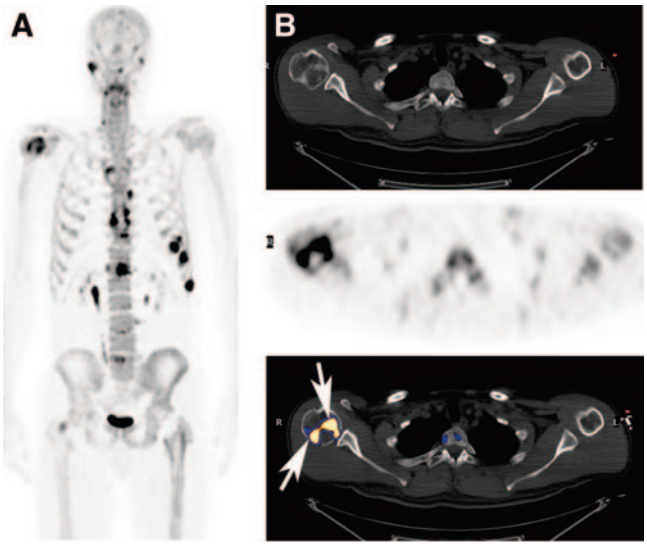

FIGURE 3. Multiple myeloma assessment by ^{18}F-fluoride PET/CT. (A) Maximum-intensity-projection image detecting multiple lesions. (B) From left to right: CT image, ^{18}F-fluoride PET image, and fused image. Increased uptake is detected in well-defined margins (arrows) of large lytic lesion detected on CT in head of right humerus.

Increased ^{18}F-fluoride uptake may also be seen in benign bone pathologies. This modality may, therefore, have a role in the evaluation of nonmalignant orthopedic problems. However, ^{18}F-fluoride is of a limited specificity in oncology, when differentiation between malignant and benign lesion is essential. It is not possible to differentiate benign from malignant ^{18}F-fluoride uptake (*26*). Because of its high sensitivity in detecting any bone pathology, ^{18}F-fluoride PET may actually be prone to a higher incidence of false-positive sites of uptake than BS. Benign lesions, which are usually not associated with increased ^{99m}Tc-MDP uptake, such as uncomplicated small subchondral cysts, were found to show increased ^{18}F-fluoride uptake (*33*). Thus, lesions detected on ^{18}F-fluoride PET may require correlation with CT or MRI (or both) for further validation (*3,34*). The use of hybrid PET/CT systems may improve the specificity of ^{18}F-fluoride PET by determining the morphology of the scintigraphic lesion on the CT data of the study (*33*).

^{18}F-FDG PET

As a glucose analog, ^{18}F-FDG gains entry into cells by glucose membrane transporter proteins that are overexpressed in many tumor cells. It is then trapped within tumor cells in which dephosphorylation is slow. ^{18}F-FDG PET assessment has the advantage of detecting both soft-tissue and skeletal disease (*27,35*). Estimates of the sensitivity of ^{18}F-FDG PET for detecting bone metastases range between 62% and 100% and the specificity ranges between 96% and 100% (*4*).

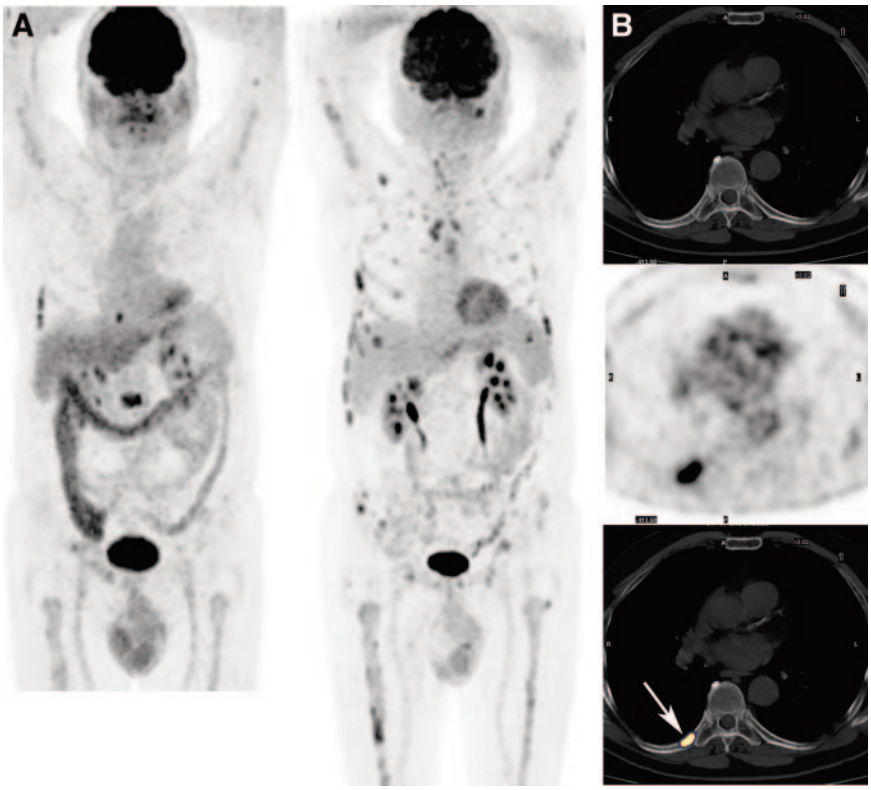

FIGURE 4. Disease progression of multiple myeloma on ^{18}F-FDG PET. (A) Two maximum-intensity-projection images 5 mo apart. Baseline study (left) was performed in patient with monoclonal gammopathy of undetermined significance who presented with vertebral plasmocytoma and spinal compression fracture. In addition to increased uptake at known spinal lesion, increased ^{18}F-FDG uptake was also detected in ribs, which appeared normal on CT data of PET/CT, probably reflecting early malignant involvement in other sites (B). Spinal lesion was treated by radiotherapy. Five months later, numerous new lesions (arrow) were identified on a repeated study, indicative of tumor progression.

The normal red marrow usually demonstrates low-intensity ^{18}F-FDG uptake, thereby assisting in detecting increased uptake in early marrow involvement before an identifiable bone reaction. These early metastases may be missed on BS and CT (Figs. 1A–1C and Fig. 4B) (*35*).

^{18}F-FDG PET has been found to be superior to BS in detecting bone involvement in various malignant diseases (*36*). Although ^{18}F-FDG PET has been reported as being appropriate for detecting all types of bone metastases—including lytic, sclerotic, and mixed lesions—accumulating data suggest that ^{18}F-FDG PET is more sensitive in detecting lytic metastases than sclerotic metastases. The latter type of metastases may show uptake of lower intensity compared with lytic lesions or even no increased uptake at all. Cook et al. reported a generally higher detection rate of bone metastases by ^{18}F-FDG PET compared with BS in patients with breast cancer. However, in a subgroup of patients who had predominately sclerotic skeletal involvement, ^{18}F-FDG uptake in bone metastases was lower and this selective group of patients had a better outcome (*37*). When interpreting a PET study, differences in ^{18}F-FDG avidity may be found in coexisting lytic and sclerotic lesions in the same patient. It is assumed that the greater avidity of ^{18}F-FDG in lytic metastases reflects the high glycolytic rate and the relative hypoxia characterizing this type of lesion, in contrast to sclerotic metastases, which are relatively acellular, less aggressive, and not prone to hypoxia (*34,35*). Using integrated PET/CT systems, each lesion may be characterized by its uptake and morphologic appearance. Metser et al. reported an increased ^{18}F-FDG uptake in 100% of metastases presenting as lytic lesions on the CT part of the PET/CT study and in 88% of the metastases presenting as sclerotic lesions (*38*).

As a rule, if the primary tumor is not ^{18}F-FDG avid, ^{18}F-FDG PET is not considered a suitable modality for staging. In these cases, failure to detect bone metastases may be unrelated to their localization in bone or to their sclerotic nature but to reflect the non–^{18}F-FDG avidity of the individual tumor. In addition, it was suggested that in the same patient, the detection rate of soft-tissue and bone metastases may be different. Some authors raised the possibility that ^{18}F-FDG PET is less sensitive for detecting bone metastases than for detecting soft-tissue metastases, whereas others reported opposite results, mainly in patients with prostate cancer, in whom the primary tumor and regional involved lymph nodes were obscured by physiologic ^{18}F-FDG uptake in the urinary tract, with better visualization of distant bone metastases (*16,39–41*).

Tumor detection with ^{18}F-FDG PET is highly susceptible to chemotherapy and radiotherapy. The use of granulocyte colony-stimulating factors in patients receiving myelosuppressive chemotherapy may induce an increased FDG uptake in red marrow, which can mask malignant infiltration (*42*). As with BS, though by a different mechanism, the flare phenomenon can also be seen on ^{18}F-FDG PET. Dehdashti et al. has reported an increase in ^{18}F-FDG uptake after the initiation of tamoxifen in responsive patients opposed to no change in ^{18}F-FDG uptake in nonresponders (*43*). It has

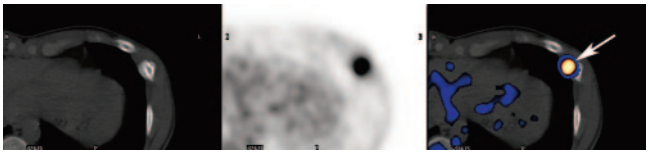

FIGURE 5. Benign ^{18}F-FDG uptake (arrow) in recent rib fracture detected on CT data of ^{18}F-FDG PET/CT in patient with lung cancer. From left to right: CT image, ^{18}F-FDG PET image, and fused image.

been proposed that this reaction is due to temporary agonist effects of the hormone on the tumor. Studies in immature female rats have shown that this initial agonist effect to tamoxifen is associated with increased tumor glucose uptake. These agonist effects may not be marked enough to result in a clinically evident flare reaction but can be documented with ^{18}F-FDG PET (*43*).

^{18}F-FDG PET is less hampered by nonspecific uptake in incidentally found benign bone lesions compared with BS or ^{18}F-fluoride PET. However, false-positive increased ^{18}F-FDG uptake may occasionally be detected in benign lesions, especially histiocytic or giant cell–containing lesions, including osteoblastoma, brown tumor, aneurysmal bone cyst, and sarcoidosis (*28,29*). Tissue histiocytic and giant cells are the in monocytes–macrophage lineage and play a central role in the host response to injury and infection. Their energy is predominately supplied by means of intracellular glucose metabolism. Although the standardized uptake value of ^{18}F-FDG in malignant bone lesions is generally higher compared with benign bone lesions, there is overlap (*29*). Based on a compartmental model, evaluation of the full ^{18}F-FDG kinetics can assist in differentiating malignant from benign bone lesions showing increased ^{18}F-FDG uptake (*28*). Using PET/CT, the benign nature of PET lesions can be sorted out on the basis of their appearance on the CT part of the study (Fig. 5) (*38*).

SPECT/CT AND PET/CT HYBRID IMAGING

Novel integrated systems composed of SPECT or PET and CT have been recently introduced into routine practice. Acquisition of the functional study (SPECT or PET) and of the morphologic study (CT) is performed without changing the patient's positioning, thus allowing for a generation of fused images on which each lesion is characterized by its tracer uptake and morphologic appearance. It has now emerged as a diagnostic tool by virtue of the relative ease with which the fused data are obtained. Some of the limitations of the previously described scintigraphic techniques may be overcome using these hybrid techniques (*16,33,38,44–47*).

The CT component of the hybrid system could be low-dose CT, integrated mainly with a SPECT γ-camera, or single-slice or multislice diagnostic CT. The data obtained by low-dose CT (140 kVp, 2.5 MA) have been reported to be valuable mainly for attenuation correction and as anatomic landmarks of the scintigraphic findings (*44*). Data obtained by diagnostic CT also provide detailed morphology of the lesions (*33,38*).

It may be difficult to accurately localize a lesion on scintigraphic studies with non–bone-specific tracers, which can detect tumor in soft tissue or bone, such as with the SPECT tracers ^{131}I, ^{111}In-somatostatin, and ^{67}Ga-citrate, and with ^{18}F-FDG used for PET (*44*). It was previously reported that bone lesions, which showed increased ^{18}F-FDG uptake, were misinterpreted as being located in soft tissue, thus yielding a lower calculated sensitivity for ^{18}F-FDG PET in detecting bone metastases, compared with BS, which defined only bone metastases (*48*). It is also difficult to assess the presence of bone metastases in the vicinity of physiologic uptake sites. For instance, it is difficult to detect skull metastases because of the high physiologic ^{18}F-FDG uptake in the adjacent brain. Some of these limitations can be overcome with SPECT/CT or PET/CT (*44,47*)

Because the routine SPECT and PET tracers used for the detection of malignant bone involvement are not tumor specific, false-positive benign lesions may show increased tracer uptake and, thus, correlation, mainly with CT, is often indicated. This limitation of the scintigraphic modalities can be overcome when using hybrid systems with CT, as the nature of many benign lesions can be determined by the CT part of the study. The ability to immediately report a benign cause of a scintigraphic finding obviates unnecessary worry on the part of the patient (Fig. 5). We performed ^{18}F-fluoride PET/CT studies on 44 patients and found a statistically significant improvement in the specificity of ^{18}F-fluoride PET/CT (97%) compared with that of ^{18}F-fluoride PET alone (72%). The high sensitivity of ^{18}F-fluoride PET was reflected by the detection of increased ^{18}F-fluoride uptake in 16 bone metastases with normal CT appearance and in 4 patients who had a false-negative BS. ^{18}F-Fluoride PET/CT was also found to be valuable in suggesting the cause of bone pain in symptomatic patients by detecting relevant benign bone lesions and by detecting a soft-tissue tumor mass invading the sacral foramen on the CT part of the study (*33*). These results are encouraging. However, more data should be accumulated, including cost considerations as well as assessment of the impact of this novel technique on patient management and outcome, to appropriately introduce ^{18}F-fluoride PET/CT for assessment of malignant bone involvement.

The results of many recently published reports suggest an improvement in the diagnostic accuracy of ^{18}F-FDG PET/CT compared with ^{18}F-FDG PET alone or even a side-by-side reading of ^{18}F PET and CT that were performed separately (*45–47*). We reported an improved specificity of ^{18}F-FDG PET/CT in detecting malignant bone involvement in the spine compared with that of ^{18}F-FDG PET alone and of CT alone. ^{18}F-FDG alone was incorrect in determining the level of abnormality within the vertebral column in 15% of lesions and in determining the part of the vertebra involved in 18% of lesions. It was also noted that

the CT part of the PET/CT study was useful for the assessment of accompanying complications: Compression of the vertebral body was identified in 5% of the vertebral lesions on CT. A major contribution of the CT part of the PET/CT study is its ability to detect soft-tissue involvement around the spine, mainly invasion of the epidural space and neural foramen, which was detected in 10% of the vertebral lesions (*38*). These lesions are neurologically significant. They may cause spinal cord compression, and early diagnosis and treatment may be essential to halt the development of permanent neurologic deficits (Fig. 2) (*49*).

^{18}F-FDG PET and PET/CT were recently reported to be of value in assessing the presence of both soft-tissue and bone metastases in patients with various malignancies, such as NSCLC, obviating the need to perform separate BS (*27,46,50*). However, if the decision is not to perform separate BS, one must be certain that the entire skeleton is assessed by PET/CT, including the lower extremities, where isolated metastases can be present, especially in patients with lung cancer.

Whole-body CT is acquired on a PET/CT study. In the case of bone abnormalities, the contrast between lesion and normal bone is clearly seen on reduced-dose CT images, obviating the need to perform separate full-dose CT for the purpose of correlation with scintigraphic skeletal findings (*33,38*).

IMAGING OF BONE INVOLVEMENT IN VARIOUS HUMAN MALIGNANCIES

Breast Cancer

The skeleton is the most common site of distant metastases in breast cancer. Bone is the first site of metastasis in 26%–50% of patients with metastatic breast cancer and it may develop during the course of the disease in 30%–85% of these patients (*4*). The vertebral column is the most common site of spread followed by the ribs. The sternum may be involved by local extension from disease in the internal mammary chain. Bone metastases of breast cancer are lytic, sclerotic, or mixed in their radiographic appearance (*1,4,37*). The risk for bone involvement, as assessed by BS, depends on the stage of the disease and varies between 0.8% and 2.6% in early stages (I and II) and between 16.8% and 40.5% in advanced stages (III and IV) (*3,4,51–53*). Therefore, routine screening of asymptomatic patients with early-stage breast cancer is not recommended anymore (*54*). BS, which is the most commonly used modality for detection of bone metastases, is indicated in patients with advanced disease or when bone involvement is clinically suspected (*51*).

The use of ^{18}F-FDG PET in patients with ^{18}F-FDG–avid breast cancer is rapidly growing, although it is not a routine staging procedure. ^{18}F-FDG PET allows for the detection of both soft-tissue and skeletal sites of disease (*55*). Cook et al. reported a higher detection rate of bone metastases by ^{18}F-FDG PET compared with BS in patients with breast cancer (*37*). The superiority of ^{18}F-FDG PET was reflected mainly in the detection of bone metastases, which were predominately lytic and had only minimal osteoblastic reaction, and, thus, were overlooked on BS (*37*). The high sensitivity of ^{18}F-FDG PET in detecting bone metastases can obviate the need to perform separate BS, although a complementary use of BS and ^{18}F-FDG PET has been suggested for optimizing the detection of both lytic and sclerotic types of metastases (*55,56*). By using PET/CT, sclerotic lesions overlooked by the PET part of the study can be identified on the CT part. In this setting, the high sensitivity of ^{18}F-FDG PET for detecting marrow and lytic lesions and the high sensitivity of CT for detecting sclerotic lesions are complementary. Noteworthy, some types of breast cancer, primarily well-differentiated histologic subtypes including some of the tubular and lobular ones, are less ^{18}F-FDG avid and so are their metastases (*55*)

^{18}F-Fluoride PET has been reported in several previous publications to be highly sensitive for detecting both lytic and blastic metastases of breast cancer (*3*). When compared with a panel of morphologic imaging techniques—including XR, CT, and MRI—^{18}F-fluoride PET was positive in small bone marrow metastases with minimal bone reaction and was associated with a change in patient management in 11.7% of the patients. Its application was, therefore, suggested in a selective group of high-risk patients with breast cancer (*3*).

A recognized effect of antiestrogen therapy commonly applied in patients with breast cancer is the "flare reaction" characterized by pain and erythema in soft-tissue lesions and increased pain in bone lesions (*20,43*). This phenomenon is presumed to reflect an initial agonist effect of the drug before its antagonist effect supervenes. Clinically, it may be difficult to differentiate the flare reaction from disease progression, mainly in patients with bone-dominant metastatic disease (*20*). Serial BS may show an increase in uptake at sites of previously detected metastases or "new" sites, which are actually responsive lytic lesions undergoing a repair process with increased osteoblastic activity. The initial agonist effect to therapy is also associated with increased tumor ^{18}F-FDG uptake. A change in ^{18}F-FDG uptake can be detected as early as 10 d after initiation of treatment compared with several weeks that are often required to make this assessment on the basis of clinical symptoms (*20,43*).

Prostate Cancer

Staging of newly diagnosed prostate cancer is essential for guiding treatment (*57*). Patients with low-risk prostate cancer are unlikely to have metastatic disease on BS. In a meta-analysis of 23 articles on the detection rate of bone metastases by BS in patients with newly diagnosed prostate cancer, the rates were 2.3% of patients with prostate-specific antigen (PSA) levels of ≤10 ng/mL, 5.3% of patients with levels between 10.1 and 19.9 ng/mL, and 16.2% of patients with PSA levels between 20 and 49.9 ng/mL (*58*). Bone metastases were detected in 6.4% of patients with

organ-confined cancer and in 49.5% of patients with locally advanced disease. Detection rates were 5.6% in patients with a Gleason score of ≤7 and 29.9% in patients with a Gleason score of ≥8. The likelihood of positive BS in asymptomatic patients with serum PSA levels of ≤20 ng% was found to be approximately 0.8% (*57*). Based on these data, patients are referred for BS mainly if they are considered to be at high risk for bone metastases, with high PSA levels, a locally advanced disease, or a high Gleason score.

BS is the most widely used method for evaluating skeletal metastases of prostate carcinoma. Based on early reports, the role of ^{18}F-FDG PET seemed to be limited in this type of malignancy as both the soft-tissue sites of disease and bone metastases were reported to be ^{18}F-FDG negative or to show only a low-intensity uptake in many patients (*59*). It has been speculated that glucose use of prostate tumor cells is not enhanced significantly compared with normal cells and that prostate cancer cells may have an alternative source of energy supply (*60*). Despite the relatively disappointing early reports, it is suggested in more recent publications that ^{18}F-FDG PET is not an unsuitable modality for assessment of patients with prostate cancer but needs to be used in selected groups of patients using adequate imaging techniques. PET/CT was suggested to overcome the problem of pelvic tumor sites being obscured by the radioactive urine (*40*). On a lesion-based analysis of 157 lesions in 17 patients with progressive metastatic prostate cancer, Morris et al. found ^{18}F-FDG PET to appropriately discriminate active bone metastatic disease from scintigraphically quiescent lesions (*61*). Using ^{18}F-FDG PET for monitoring the response to treatment, a decline in tumor glucose uptake was measured as early as 48 h after androgen withdrawal, preceding any change in tumor volume or in PSA levels (*40*). Other PET tracers suggested for assessment of prostate cancer include ^{11}C- or ^{18}F-labeled choline and acetate, ^{11}C-methionine, ^{18}F-fluorodihydrotestosterone, and ^{18}F-fluoride (*40,41*). The latter may be highly sensitive for detecting bone metastases in patients with prostate cancer; however, further validation of the added value of ^{18}F-fluoride PET compared with BS is needed (*60,62*).

Lung Cancer

Surgical resection offers the highest probability of a favorable outcome in patients with NSCLC. However, the survival of patients who undergo surgery remains low, probably because of presurgical understaging. Bone metastases are diagnosed at initial presentation in 3.4%–60% of patients with NSCLC. Bone pain is usually considered an indicator of skeletal metastases, but up to 40% of lung cancer patients with proven bone metastases are asymptomatic (*27,46,50,63*). Clinical staging at presentation has been performed by means of CT of the thorax through the liver and adrenals, CT or MRI of the brain, and BS for assessment of bone involvement. This staging algorithm remains the most commonly used in places where ^{18}F-FDG PET is not a routine staging modality of lung cancer. Including SPECT in the acquisition protocol of BS could improve the diagnostic accuracy of BS in detecting bone metastases in patients with lung cancer. If necessary, BS can be complemented by CT or regional MRI for further assessment of unclear lesions (*32*). ^{18}F-FDG PET and PET/CT were recently reported to be of value in assessing the presence of soft-tissue and bone spread in patients with NSCLC, obviating the need to perform separate BS (*27,46,50*). In a study on 110 consecutive patients with NSCLC, Bury et al. showed ^{18}F-FDG PET to be superior to BS in detecting bone metastases, with an accuracy of 96% and 66% for each of the modalities, respectively. They reported that ^{18}F-FDG PET had a high positive predictive value and a lower false-positive rate compared with BS (*63*).

Lymphoma

Primary bone involvement occurs in 3%–5% of the patients with non-Hodgkin's lymphoma and 25% of them have secondary bone involvement. Primary bone involvement is rare in Hodgkin's disease (HD). Secondary bone involvement occurs in 5%–20% of patients with HD during the course of the disease but in only 1%–4% at presentation. Lymphomatous bone involvement is the result of hematogenous spread or direct extension from adjacent soft-tissue disease. Bone involvement upgrades disease to stage IV and is indicative of an aggressive disease with a poor outcome. Extension of disease from adjacent disease in the soft tissue to bone, however, does not alter staging. The radiographic features of bone lymphoma are nonspecific. Lesions may be solitary or, more commonly, polyostotic. They are predominately osteolytic but may be sclerotic or mixed. Lysis is the rule in the vertebral column, but patchy sclerosis and "ivory vertebrae" are frequently seen (*64,65*).

^{67}Ga scintigraphy has been found to be a sensitive imaging modality for detecting bone involvement of lymphoma, mainly with the administration of high doses of ^{67}Ga and the use of SPECT. Both lytic and sclerotic lesions were reported to be ^{67}Ga avid. The lymphoma-seeking properties of ^{67}Ga rather than its bone-seeking properties are presumably the primary cause of increased ^{67}Ga uptake in lymphoma involving the bone (*66,67*). In a previous publication by Israel et al. (*67*), ^{67}Ga SPECT was found to be both sensitive and specific for monitoring the response of bone lymphoma to therapy. Persistent increased ^{67}Ga uptake in a skeletal disease site at the end of therapy has been shown to indicate active disease, whereas a negative ^{67}Ga study suggests complete response and a favorable outcome, regardless of its appearance on follow-up CT, which may remain abnormal even when the disease is "burnt out" (*67*).

Lymphoma involvement is commonly marrow based. MRI is a sensitive modality for detecting marrow infiltration but it is not a routine modality for staging of lymphoma. In recent years, ^{18}F-FDG PET has been used for staging and for monitoring the response to therapy in patients with lymphoma, replacing the use of ^{67}Ga scintigraphy in many centers. ^{18}F-FDG PET can detect early marrow infiltration

and, therefore, is of sensitivity superior to that of BS for assessment of early bone involvement in lymphoma (*68,69*). ^{18}F-FDG PET is also more sensitive than CT for detecting bone involvement. When performed by means of a hybrid PET/CT system, unexpected bone involvement can be identified by increased ^{18}F-FDG uptake with either corresponding abnormalities on the CT data of the study or with a normal CT appearance when bone involvement is early—that is, before identifiable bone destruction. The delay in detecting lymphomatous bone involvement on CT reflects its relatively low sensitivity in assessing malignant marrow infiltration and the fact that detection of malignant bone involvement on CT depends on the presence of a considerable amount of bone destruction (*1,67*). A valuable contribution of the CT data of PET/CT in lymphoma patients is its capacity to detect soft-tissue paravertebral masses as well as epidural masses and neural foramen invasion, which may accompany vertebral disease more commonly in lymphoma patients (Fig. 2) (*38,64,65*).

The pattern of marrow involvement by lymphoma is often patchy. A "blind" marrow sampling may result in false-negative results if the biopsy site is not infiltrated by lymphoma. It has been suggested that ^{18}F-FDG PET could replace the blind procedure or may be used to guide the appropriate biopsy site (*69*). Marrow involvement is uncommon at presentation in HD and, therefore, marrow biopsy is not routinely performed as part of the initial staging in all patients (*64*). During the course of the disease, however, 5%–32% of patients develop bone marrow involvement (*69–71*). ^{18}F-FDG PET can identify patients with HD who are at high risk to have marrow involvement and in whom marrow sampling is indicated as part of the staging algorithm.

Assessment by ^{18}F-FDG PET of the activity of disease in the marrow after therapy is hampered by the resemblance of active lymphoma infiltration to reactive marrow changes and by the effect of chemotherapy and granulocyte colony-stimulating factors on the distribution of the tracer in the marrow (*42,70*).

Multiple Myeloma (MM)

MM is a clonal B-lymphocyte neoplasm of plasma cells. It accounts for 1% of all malignant diseases and represents 10% of hematologic malignancies. The hallmark of MM is the presence of a monoclonal protein, M protein, produced by the abnormal plasma cells in the blood or urine. Once the diagnosis is suspected, a radiographic skeletal survey and bone marrow aspiration and biopsy are performed (*9*). The effects of abnormal plasma cells are excessive bone resorption and inhibition of bone formation. The clinical presentations of MM are bone pain, severe osteopenia, and skeletal fractures, including multilevel spinal cord compression fractures. In clinical practice of myeloma patients, imaging is complementary to measurements of biochemical markers of bone turnover. The latter were reported to reflect the disease activity in bone and the extent of disease and to be helpful in identifying patients likely to respond to bisphosphonate treatment (*72*).

XR is the primary imaging modality for detecting bone changes in MM and is included in the Durie–Salmon clinical staging criteria of newly diagnosed MM. Its main limitation is that approximately 50% bone destruction must occur before there is radiographic evidence of a bone lesion. Four distinct forms of myeloma have been described on XR: a solitary lytic lesion (plasmocytoma), diffuse skeletal involvement (myelomatosis) presenting as osteolytic lesions with discrete margins, diffuse skeletal osteopenia without well-defined lytic lesions, and sclerosing myeloma.

CT is a sensitive tool for detecting the bone-destructive effects of MM (Fig. 3B). MM findings that can be detected on CT include lytic lesions, expansile lesions with soft-tissue masses, diffuse osteopenia, and fractures (*73*).

BS is considered less sensitive than XR and CT due to the presence of only minimal osteoblastic activity in most myeloma lesions, which are predominately lytic (*74*). Almost half of the abnormal sites of disease identified radiographically were reported to be overlooked by BS. Scintigraphic abnormalities associated with myeloma may appear as increased sites of ^{99m}Tc-MDP uptake, mainly in the presence of fractures, or as "cold" lesions. Soft-tissue uptake may be detected in association with calcification within a plasmocytoma or secondary amyloidosis (*9*). Scintigraphy with ^{99m}Tc-sestamibi has been shown to assist in demonstrating the extent of disease. At follow-up, its use could be limited in the presence of a multidrug resistance, which blocks the accumulation of ^{99m}Tc-sestamibi in myeloma cells (*75*).

MRI has recently been used in patients with MM for assessment of the actual tumor burden in the marrow and the presence of accompanying complications. Spinal compression fractures caused by bone destruction or by a mass occur in 55%–70% of patients with MM. The image features of MM on MRI, however, are not specific and can also be found in other disease processes, such as drug-induced reactive marrow or increased hematopoiesis in patients with severe anemia (*76*).

Experience with ^{18}F-FDG PET in patients with MM is rapidly expanding. Previous reports have shown that ^{18}F-FDG PET can detect unexpected medullary and extramedullary sites of disease missed by XR, CT, and BS (Fig. 4) (*77–79*). In a series of 43 patients, Shirrmeister et al. reported a sensitivity of 93% for detection of osteolytic MM by ^{18}F-FDG PET (*77*). Durie et al. (*78*) assessed the role of ^{18}F-FDG PET in 66 patients with MM and monoclonal gammopathy of undetermined significance (MGUS). Their results suggested that positive ^{18}F-FDG PET reliably detects active MM, whereas a negative study strongly supports the diagnosis of MGUS (Fig. 4). The authors concluded that detection of extramedullary sites of disease and residual ^{18}F-FDG uptake, on a follow-up study after stem cell transplantation, are poor prognostic factors.

MONITORING RESPONSE TO TREATMENT

No general consensus has been reached on the optimal imaging algorithm for monitoring the response of malignant bone involvement to therapy. Follow-up protocols may vary for different malignancies.

Bone disease is considered unmeasurable. Determining complete or partial response can be difficult, mainly because it is not always possible to differentiate between residual tumor and repair process. Even when clinical complete remission has been achieved, "normalization" of bone may be delayed after the disappearance of other soft-tissue sites of the disease. Moreover, bone may remain morphologically abnormal even when the disease is "burnt out" (*40*). These difficulties are particularly relevant when using imaging modalities that detect malignant bone involvement based on the presence of bone destruction or reactive bone remodeling such as CT, BS, and ^{18}F-fluoride PET. For that matter, modalities that detect malignant involvement by a direct visualization of the tumor tissue, such as ^{18}F-FDG PET, may be beneficial since response can be assessed by recording the change in ^{18}F-FDG uptake in the skeletal lesions. The latter technique was reported to be well correlated with the clinical response and tumor markers in patients with bone-dominant breast cancer (*80*).

CONCLUSION

Various morphologic and scintigraphic imaging modalities can detect malignant bone involvement. Each of the modalities has advantages and limitations and their role may vary in patients with different malignant diseases. MRI and ^{18}F-FDG PET can detect malignant marrow involvement early in the course of the disease before identifiable bone destruction or reactive osteoblastic changes occur and, thus, may precede CT and BS in identifying the presence of malignant bone involvement. Although ^{18}F-fluoride uptake depends on regional blood flow and osteoblastic activity, similar to ^{99m}Tc-MDP, the better spatial resolution of PET and the favorable pharmacokinetic characteristics of ^{18}F-fluoride make ^{18}F-fluoride PET a more sensitive modality for detecting both lytic and blastic lesions. ^{18}F-Fluoride PET is, however, not a routine modality. BS remains the most commonly used procedure for assessing the presence of bone metastases because of its high sensitivity, availability, and relatively low cost. The performance of SPECT significantly improves its diagnostic accuracy. ^{18}F-FDG PET has been introduced in staging and follow-up of various ^{18}F-FDG–avid malignancies, obviating the need to perform a separate study with another modality for assessment of bone involvement.

CT and MRI depict detailed anatomic changes and can identify complications of bone metastases. CT is preferable for assessing bone morphology, whereas MRI is superior for detecting early marrow infiltration and epidural masses. Scintigraphic findings may require further correlation with morphologic modalities, mainly with CT. Novel hybrid techniques that allow the acquisition of SPECT or PET and CT at the same clinical setting and the generation of fused functional–anatomic data have been found to improve the diagnostic accuracy of scintigraphic techniques in detecting malignant bone involvement. Finally, accompanying complications in the bone and soft tissue can also be identified from the CT data of the study.

ACKNOWLEDGMENT

The author thanks Dr. Gennady Lievshitz for preparing the figures.

REFERENCES

1. Padhani A, Husband J. Bone metastases. In: Husband JES, Reznek RH, eds. *Imaging in Oncology*. Oxford, U.K.: Isis Medical Media Ltd.; 1998:765–787.
2. Rybak LD, Rosenthal DI. Radiological imaging for the diagnosis of bone metastases. *Q J Nucl Med.* 2001;45:53–64.
3. Schirrmeister H, Guhlnamm A, Kotzerke J, et al. Early detection and accurate description of extent of metastatic bone disease in breast cancer with fluoride ion and positron emission tomography. *J Clin Oncol.* 1999;17:2381–2389.
4. Hamaoka T, Madewell JE, Podoloff DA, Hortobagyi GN, Ueno NT. Bone imaging in metastatic breast cancer. *J Clin Oncol.* 2004;22:2942–2953.
5. Morgan-Parkes JH. Metastases: mechanisms, pathways, and cascades. *AJR.* 1995;164:1075–1082.
6. Kricun ME. Red-yellow marrow conversion: its effect on the location of some solitary bone lesions. *Skeletal Radiol.* 1985;14:10–19.
7. Blake GM, Park-Holohan SJ, Cook GJ, Fogelman I. Quantitative studies of bone with the use of ^{18}F-fluoride and ^{99m}Tc-methylene diphosphonate. *Semin Nucl Med.* 2001;31:28–49.
8. Bellamy EA, Nicholas D, Ward M, et al. Comparison of computed tomography and conventional radiology in the assessment of treatment response of lytic bony metastases in patients with carcinoma of the breast. *Clin Radiol.* 1987;38:351–355.
9. Angtuaco EJC, Fassas ABT, Walker R, Sethi RH, Barlogie B. Multiple myeloma: clinical review and diagnostic imaging. *Radiology.* 2004;231:11–23.
10. Muindi J, Coombes RC, Golding S, et al. The role of computed tomography in the detection of bone metastases in breast cancer patients. *Br J Radiol.* 1983;56:233–236.
11. Karnholz R, Sze G. Current imaging in spinal metastatic disease. *Semin Oncol.* 1991;18:158–169.
12. Vogler JB 3rd, Murphy WA. Bone marrow imaging. *Radiology.* 1988;168:679–693.
13. Tryciecky EW, Gottschalk A, Ludema K. Oncologic imaging: interactions of nuclear medicine with CT and MRI using the bone scan as a model. *Semin Nucl Med.* 1997;27:142–151.
14. Vanel D, Dromain C, Tardivon A. MRI of bone marrow disorders. *Eur Radiol.* 2000;10:224–229.
15. Daldrup-Link HE, Franzius C, Link TM, et al. Whole body MR imaging for detection of bone metastases in children and young adults. *AJR.* 2001;177:229–236.
16. Antoch G, Vogt FM, Freudenberg LS, et al. Whole-body dual-modality PET/CT and whole-body MRI for tumor staging in oncology. *JAMA.* 2003;290:3199–3206.
17. Schneider JA, Divgi CR, Scott AM, et al. Flare on bone scintigraphy following Taxol chemotherapy for metastatic breast cancer. *J Nucl Med.* 1994;35:1748–1752.
18. Coleman RE, Mashiter G, Whitaker KB, et al. Bone scan flare predicts successful systemic therapy for bone metastases. *J Nucl Med.* 1988;29:1354–1359.
19. Vogel CL, Schoenfelder J, Shemano I, et al. Worsening bone scan in the evaluation of antitumor response during hormonal therapy of breast cancer. *J Clin Oncol.* 1995;13:1123–1128.
20. Mortimer JE, Dehdashti F, Siegel BA. Metabolic flare: indicator of hormone responsiveness in advanced breast cancer. *J Clin Oncol.* 2001;19:2797–2803.
21. Gates GF. SPECT bone scanning of the spine. *Semin Nucl Med.* 1998;28:78–94.
22. Savelli G, Maffioli L, Maccauro M, De Deckere E, Bombardieri E. Bone scintigraphy and the added value of SPECT (single photon emission tomography) in detecting skeletal lesions. *Q J Nucl Med.* 2001;45:27–37.
23. Even-Sapir E, Martin RH, Barnes DC, Pringle CR, Iles SE, Mitchell MJ. Role of SPECT in differentiating malignant from benign lesions in the lower thoracic and lumbar vertebrae. *Radiology.* 1993;187:193–198.
24. Algra PR, Heimans JJ, Valk J, Nauta JJ, Lachniet M, Van Kooten B. Do metastases in vertebrae begin in the body or the pedicles? Imaging study in 45 patients. *AJR.* 1992;158:1275–1279.

25. Yuh WTC, Zachar CK, Barloon TJ, Sato Y, Sickles WJ, Hawes DR. Vertebral compression fractures: distinction between benign and malignant causes with MR imaging. *Radiology.* 1989;172:215–218.
26. Cook GJ, Fogelman I. The role of positron emission tomography in skeletal disease. *Semin Nucl Med.* 2001;31:50–61.
27. Rohren EM, Turkington TG, Coleman RE. Clinical applications of PET in oncology. *Radiology.* 2004;231:305–332.
28. Dimitrakopoulou-Strauss A, Strauss LG, Heichel T, et al. The role of quantitative ^{18}F-FDG PET studies for the differentiation of malignant and benign bone lesions. *J Nucl Med.* 2002;43:510–518.
29. Aoki J, Watanabe H, Shinozaki T, et al. FDG PET of primary benign and malignant bone tumors: standardized uptake value in 52 lesions. *Radiology.* 2001;219:774–777.
30. Schiepers C, Nuytes J, Bormans G, et al. Fluoride kinetics of the axial skeleton measured in vivo with fluorine-18-fluoride PET. *J Nucl Med.* 1997;38:1970–1976.
31. Blau M, Nagler W, Bender MA. A new isotope for bone scanning. *J Nucl Med.* 1962;3:332–334.
32. Schirrmeister H, Glatting G, Hetzel J, et al. Prospective evaluation of clinical value of planar bone scan, SPECT and ^{18}F-labeled NaF PET in newly diagnosed lung cancer. *J Nucl Med.* 2001;42:1800–1804.
33. Even-Sapir E, Metser U, Flusser G, et al. Assessment of malignant skeletal disease with ^{18}F-fluoride PET/CT. *J Nucl Med.* 2004;45:272–278.
34. Petren-Mallmin M, Andrasson I, Ljunggren O, et al. Skeletal metastases from breast cancer: uptake of F18-fluoride measured with positron emission tomography in correlation with CT. *Skelet Radiol.* 1998;27:72–76.
35. Cook GJ, Fogelman I. The role of positron emission tomography in the management of bone metastases. *Cancer.* 2000;88:2927–2933.
36. Franzius F, Sciuk J, Daldrup-Link HE, Jurgens H, Schober O. FDG-PET for detection of osseous metastases from malignant primary bone tumours: comparison with bone scintigraphy. *Eur J Nucl Med.* 2000;27:1305–1311.
37. Cook GJ, Houston S, Rubens R, Maisey MN, Fogelman I. Detection of bone metastases in breast cancer by ^{18}FDG PET: differing metabolic activity in osteoblastic and osteolytic lesions. *J Clin Oncol.* 1998;16:3375–3379.
38. Metser U, Lerman H, Blank A, Lievshitz G, Bokstein F, Even-Sapir E. Malignant involvement of the spine: assessment by ^{18}F- fluorodeoxyglucose PET/CT. *J Nucl Med.* 2004;45:279–284.
39. Moon DH, Maddahi J, Silverman DHS. Accuracy of whole-body [fluorine-18]-FDG-PET for the detection of recurrent or metastatic breast carcinoma. *J Nucl Med.* 1998;39:431–435.
40. Schoder H, Larson SM. Positron emission tomography for prostate, bladder, and renal cancer. *Semin Nucl Med.* 2004;34:274–292.
41. Fricke E, Machtens S, Hofmann M, et al. Positron emission tomography with ^{11}C-acetate and ^{18}F-FDG in prostate cancer patients. *Eur J Nucl Med Mol Imaging.* 2003;30:607–611.
42. Clamp A, Danson S, Nguyen H, Cole D, Clemons M. Assessment of therapeutic response in patients with metastatic bone disease. *Lancet Oncol.* 2004;5:607–616.
43. Dehdashti F, Flanagan FL, Mortimer JE. Positron emission tomographic assessment of "metabolic flare" to predict response of metastatic breast cancer to antiestrogen therapy. *Eur J Nucl Med.* 1999;26:51–56.
44. Keidar Z, Israel O, Krausz Y. SPECT/CT in tumor imaging: technical aspects and clinical applications. *Semin Nucl Med.* 2003;33:205–218.
45. Bar-Shalom R, Yefremov N, Guralnik L, et al. Clinical performance of PET/CT in evaluation of cancer: additional value for diagnostic imaging and patient management. *J Nucl Med.* 2003;44:1200–1209.
46. Lardinois D, Weder W, Hany TF, et al. Staging of non-small-cell lung cancer with integrated positron-emission tomography and computed tomography. *N Engl J Med.* 2003;348:2500–2507.
47. Kostakoglu L, Hardoff R, Mirtcheva R, Goldsmith SJ. PET/CT fusion imaging in differentiating physiologic from pathologic FDG uptake. *Radiographics.* 2004; 24:1411–1431.
48. Gayed I, Vu T, Johnson M, Macapinlac H, Podoloff D. Comparison of bone and 2-deoxy-2-[^{18}F]fluoro-D-glucose positron emission tomography in the evaluation of bony metastases in lung cancer. *Mol Imaging Biol.* 2003;5:26–31.
49. Van Goethem JW, van den Hauwe L, Ozsarlak O, De Schepper AM, Parizel PM. Spinal tumors. *Eur J Radiol.* 2004;50:159–176.
50. Cheran SK, Herndon JE, Patz EF. Comparison of whole-body FDG-PET to bone scan for detection of bone metastases in patients with a new diagnosis of lung cancer. *Lung Cancer.* 2004;44:317–325.
51. Maffioli L, Florimonte L, Pagani L, Butti I, Roca I. Breast cancer: diagnostic and therapeutic options. *Eur J Nucl Med Mol Imaging.* 2004;31(suppl 1):S143–S148.
52. Coleman RE, Rubens RD, Fogelman I. Reappraisal of the baseline bone scan in breast cancer. *J Nucl Med.* 1988;29:1045–1049.
53. Yeh KA, Fortunato L, Ridge JA, et al. Routine bone scanning in patients with T1 and T2 breast cancer: a waste of money. *Ann Surg Oncol.* 1995;2:319–324.
54. Smith TJ, Davidson NE, Schapira DV, et al. American Society of Clinical Oncology 1998 update of recommended breast cancer surveillance guidelines. *J Clin Oncol.* 1999;17:1080–1082.
55. Eubank WB, Mankoff DA. Current and future uses of positron emission tomography in breast cancer imaging. *Semin Nucl Med.* 2004;34:224–240.
56. Gallowitsch HJ, Kresnik E, Gasser J, et al. F-18 fluorodeoxyglucose positron-emission tomography in the diagnosis of tumor recurrence and metastases in the follow-up of patients with breast carcinoma: a comparison to conventional imaging. *Invest Radiol.* 2003;38:250–256.
57. Lee N, Fawaaz R, Olsson CA, et al. Which patients with newly diagnosed prostate cancer need a radionuclide bone scan? An analysis based on 631 patients. *Int J Radiat Oncol Biol Phys.* 2000;48:1443–1446.
58. Abuzallouf S, Dayes I, Lukka H. Baseline staging of newly diagnosed prostate cancer: a summary of the literature. *J Urol.* 2004;171:2122–2127.
59. Shreve PD, Grossman HB, Gross MD, Wahl RL. Metastatic prostate cancer: initial finding of PET 2-deoxyglucose-[F-18]fluoro-D-glucose. *Radiology.* 1996; 199:751–756.
60. Oyen WJG, Witjes JA, Corstens FHM. Nuclear medicine techniques for the diagnosis and therapy of prostate carcinoma. *Eur Urol.* 2001;40:294–299.
61. Morris MJ, Akhurst T, Osman I, et al. Fluorinated deoxyglucose positron emission tomography imaging in progressive metastatic prostate cancer. *Urology.* 2002;59:913–918.
62. Schirrmeister H, Guhlmann A, Elsner K, et al. Sensitivity in detecting osseous lesions depends on anatomic localization: planar bone scintigraphy versus ^{18}F PET. *J Nucl Med.* 1999;40:1623–1629.
63. Bury T, Barreto A, Daenen F, Barthelemy N, Ghaya B, Rigo P. Fluorine-18 deoxyglucose positron emission tomography for the detection of bone metastases in patients with non-small cell lung cancer. *Eur J Nucl Med.* 1998;25:1244–1247.
64. Guermazi A, Brice P, de Kerviler E, et al. Extranodal Hodgkin disease: spectrum of disease. *Radiographics.* 2001;21:161–179.
65. Edeiken-Monroe B, Edeiken J, Kim EE. Radiologic concepts of lymphoma of bone. *Radiol Clin North Am.* 1990;28:841–864.
66. Bar-Shalom R, Israel O, Epelbaum R, et al. Gallium-67 scintigraphy in lymphoma with bone involvement. *J Nucl Med.* 1995;36:446–450.
67. Israel O, Mekel M, Bar-Shalom R, et al. Bone lymphoma: ^{67}Ga scintigraphy and CT for prediction of outcome after treatment. *J Nucl Med.* 2002;43:1295–1303.
68. Moog F, Kotzerke J, Reske SN. FDG PET can replace bone scintigraphy in primary staging of malignant lymphoma. *J Nucl Med.* 1999;40:1407–1413.
69. Moog F, Bangrter M, Kotzerke J, et al. 18-F-fluorodeoxyglucose-positron emission tomography as a new approach to detect lymphomatous bone marrow. *J Clin Oncol.* 1998;16:603–609.
70. Cook GJ, Fogelman I, Maisey MN. Normal physiological and benign pathological variants of 18-fluoro-2-deoxyglucose positron-emission tomography scanning: potential for error interpretation. *Semin Nucl Med.* 1996;26:308–314.
71. Carr R, Barrington SF, Madan B, et al. Detecion of lymphoma in bone marrow by whole-body positron emission tomography. *Blood.* 1998;91:3340–3346.
72. Terpos E, Politou M, Rahemtulla A. The role of markers of bone remodeling in multiple myeloma. *Blood Rev.* 2005;19:125–142.
73. Avva R, Vanhemert R, Barlogie B, et al. CT-guided biopsy of focal lesions in patients with multiple myeloma may reveal new and more aggressive cytogenetic abnormalities. *AJNR.* 2001;22:781–785.
74. Woolfenden JM, Pitt MJ, Durie BGM, Moon TE. Comparison of bone scintigraphy and radiology in multiple myeloma. *Radiology.* 1980;134:723–728.
75. Pace L, Catalano L, Del Vecchio S, et al. Predictive value of technetium-99m sestamibi in patients with multiple myeloma and potential role in the follow-up. *Eur J Nucl Med.* 2001;28:304–312.
76. Lecouvet FE, Malghem J, Michaux L, et al. Vertebral compression fractures in multiple myeloma. II. Assessment of fracture risk with MR imaging of spinal bone marrow. *Radiology.* 1997;204:201–205.
77. Schirrmeister H, Bommer M, Buck AK, et al. Initial results in the assessment of multiple myeloma using F-18 FDG PET. *Eur J Nucl Med Mol Imaging.* 2002; 29:361–366.
78. Durie BGM, Waxman AD, D'Agnolo A, Williams CM. Whole-body ^{18}F-FDG PET identifies high-risk myeloma. *J Nucl Med.* 2002;43:1457–1463.
79. el-Shirbiny AM, Yeung H, Imbriaco M, Michaeli J, Macapinlac H, Larson SM. Technetium-99m-MIBI versus fluorine-18-FDG in diffuse multiple myeloma. *J Nucl Med.* 1997;38:1208–1210.
80. Stafford SE, Gralow JR, Schubert EK. Use of serial FDG-PET to measure the response of bone-dominant breast cancer to therapy. *Acad Radiol.* 2001;9:913–921.